

T004 DATA-DRIVEN IMAGING WITH SECOND-ORDER TRAVELTIME APPROXIMATIONS

J. MANN and Y. ZHANG

Geophysical Institute, University of Karlsruhe, Hertzstr. 16, 76187 Karlsruhe, Germany

Summary. Starting with the general concept of second-order traveltime approximations for seismic reflection imaging, we discuss the number of free parameters, i. e., spatial derivatives of the traveltime, for different acquisition geometries and processing approaches ranging from the most general multi-parameter problem down to the well-known single-parameter approach used in the common-midpoint stack. With the help of the near-surface velocity, these derivatives can be related to spatial properties of hypothetical wavefronts observed at the acquisition surface. This constitutes the basis for a number of recently introduced data-driven imaging methods that differ in the derivation and representation of their traveltime approximations. Our aim is to present the current state of the art of one of the available implementations, the Common-Reflection-Surface Stack, followed by two application examples that demonstrate the advantages of the formulation in terms of wavefront properties.

Introduction. Seismic reflection imaging methods based on traveltime approximations of second order have been commonly used for decades: the classic common-midpoint (CMP) stack or the normal moveout(NMO)/dip moveout(DMO)/stack sequence can be seen as such processes, although their data-driven aspects are often not fully exploited. In recent years, several methods emerged that overcome many of the limitations of the classic approaches and go beyond the restriction to certain subsets of the pre-stack data. Instead of only one parameter, the stacking velocity, an entire set of kinematic wavefield attributes allows to locally approximate the reflection response of the subsurface for arbitrary source and receiver configurations. These attributes, associated with first and second spatial derivatives of the traveltime, can be directly determined from the pre-stack data such that no explicit parameterization of the depth model is required. The physical interpretation of the attributes in terms of propagation directions and wavefront curvatures provides information that serves for various applications like inversion, migration etc. Thus, merely stacking the pre-stack data is only one aspect in data-driven imaging based on second-order traveltime approximations.

Basic concepts. A second-order traveltime approximation with respect to an arbitrarily chosen point P on a reflection event in the pre-stack data can be described by any (hyper-)surface that includes the point P itself and coincides with the actual reflection event with respect to its first and second spatial derivatives at P . The surface fitting best the actual reflection events, together with the spatial derivatives that serve as its parameters, can be determined by means of a coherence analysis within an appropriate aperture in the pre-stack data. In the most general case of 3-D acquisition with full azimuth coverage, the pre-stack data consists of a 5-D hyper-volume spanned by the time t , the source coordinates \vec{s} , and the receiver coordinates \vec{g} , both considered to be located on a plane measurement surface for the moment. Thus, four first derivatives and nine second derivatives are required to fully describe a second order approximation of the traveltime. For the corresponding 2.5-D problem, this reduces to two first and three second derivatives. If we express the coordinates in terms of midpoint $\vec{\xi} = (\vec{g} + \vec{s})/2$ and half-offset $\vec{h} = (\vec{g} - \vec{s})/2$, further simplifications occur if we address the problem of zero-offset (ZO) simulation, where shot and receiver coordinates of P coincide: due to the reciprocity of traveltimes, the first derivatives with respect to \vec{h} and the mixed second derivatives including \vec{h} vanish. Accordingly, two first derivatives and six second derivatives remain in 3-D,

and one first and two second derivatives in 2.5-D. Restricting our traveltimes approximation in the latter case to the CMP gathers only, we end up with a single second derivative which is traditionally interpreted in terms of stacking velocity—simply a special case of the general second order approach. If only subsets of the full 5-D data hyper-volume are acquired and/or processed, the number of required derivatives obviously also reduces. The following table summarizes the number of dimensions of the pre-stack data volume and the number of required derivatives for different acquisition geometries. The numbers in parentheses refer to the special case of ZO simulation.

Acquisition geometry	Data space	Number of derivatives
3-D, full azimuth coverage	5-D	13 (8)
3-D, narrow azimuth coverage	4-D	7 (6)
2-D line	3-D	5 (3)

The representation of the stacking surface can be chosen in several ways. Depending on the derivation of the traveltimes approximation, either geometrical or by means of the ray propagator formalism of paraxial ray theory, one obtains double-square-root expressions like in Multifocusing (Berkovitch et al., 1994; Landa et al., 1999) or different kinds of quadrics of parabolic and hyperbolic form (Schleicher et al., 1993; Höcht et al., 1999). Although some of these expressions are exact for very simple situations, it is not evident which of these alternatives generally leads to the best possible results.

Physical interpretation of the derivatives. So far, the entire imaging problem has been described in terms of traveltimes derivatives without any physical interpretation. However, such an interpretation is mandatory if we want to be able to decide which values of the derivatives are reasonable for (primary) reflection events and, thus, worthwhile to be considered. Furthermore, this approach provides information about the properties of the reflectors and their overburden and allows additional generalizations that account, e. g., for the topography of the acquisition surface. Introducing a near-surface velocity v_0 , assumed to be known and almost constant inside the aperture, we can readily relate the first derivatives (often also called horizontal slownesses) to the incidence and emergence directions of wavefronts originating from hypothetical experiments, measured at the known source and receiver positions associated with P . Accordingly, the second derivatives can be related to the curvatures of these wavefronts. In other words, v_0 is the link between the traveltimes derivatives and spatial properties of wavefronts at the acquisition surface. In the hypothetical experiments, wave propagation is considered along a central ray connecting the source and receiver associated with P . Nevertheless, the properties of the actual central ray are not required and no ray tracing is involved. There are various real and hypothetical experiments that can be associated with the spatial derivatives of traveltimes. For the sake of simplicity, we restrict ourselves to the maybe simplest interpretation that can be used for the case of ZO simulation: here, the second derivatives with respect to \vec{h} can be related to a wavefront emanating from a point source at the (unknown) reflection point in depth (the so-called NIP wave experiment), whereas the derivatives with respect to $\vec{\xi}$ locally describe a wavefront originating from an exploding reflector (the so-called normal wave experiment). The first derivatives with respect to $\vec{\xi}$ enter into the description of both wavefronts. Obviously, the concept of such experiments is well suited for inversion algorithms, either by downward propagation of the wavefronts until they satisfy an imaging condition (for the above example, the focusing of the NIP wavefront at time zero) in a generalized Dix-type inversion (Biloti et al., 2002), or by tomographic approaches that are based on the forward-modeling of the wavefronts (Duveneck, 2003).

Implementation strategies. The determination of the traveltimes derivatives (or, alternatively, of the wavefield attributes) from the pre-stack data is a multi-parameter non-linear global optimization problem. The crucial task is to solve this problem in a reasonable amount of time while preserving a sufficient accuracy of the results. There is no unique way to address this for all kinds of acquisition geometries. Nevertheless, the use of subsets of the pre-stack data with sufficient coverage to determine the wavefield attributes step by step appears to be an appropriate strategy in many cases. For instance, the existing ZO implementations of the CRS stack in 2-D and 3-D determine the wavefield attributes step by step starting with CMP gath-

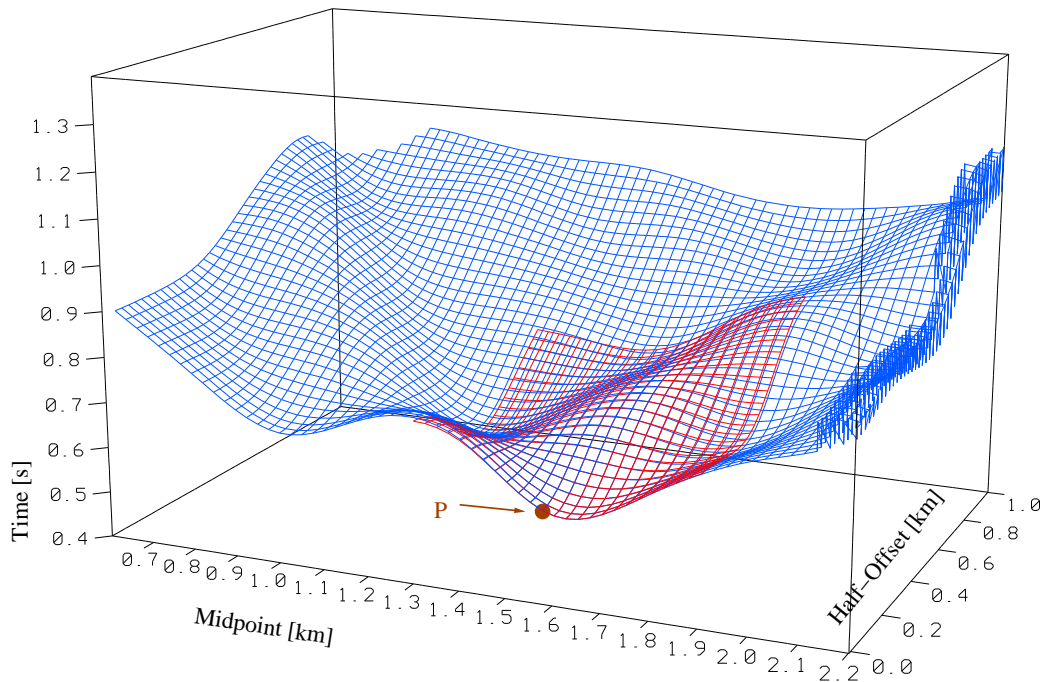


Figure 1: Reflection event (blue) in the (t, ξ, h) -domain with non-hyperbolic moveout due to topography. The wavefield attributes allow to consider the topography such that the complex event can still be approximated with a generalized second-order traveltimes approximation (red).

ers/volumes followed by an analysis of the resulting ZO section/volume. For the more general problem of non-zero offsets, similar strategies are applied in the common-shot, common-offset, and CMP gathers. For certain acquisition geometries, the attribute search for the 3-D case can be partly or entirely decomposed into 2-D configurations, again significantly simplifying the optimization problem to be solved.

The relevant traveltimes expressions are available for the most general case, i. e., arbitrary offset and 3-D acquisition with full azimuth coverage. The topography of the acquisition surface can be consistently considered from the very beginning. Concerning implementation and application, the CRS stack is currently available for 2-D ZO simulation (including topography and redatuming to a plane datum), 2-D finite-offset simulation, and 3-D ZO simulation.

Application examples. As already mentioned above, the physical interpretation of the derivatives in terms of wavefield attributes can be used for various applications, either during the stacking or in subsequent processes like inversion. In the scope of this abstract, we focus on the explicit consideration of topography in the 2-D ZO CRS stack. To demonstrate this technique, we used a simple synthetic 2-D model with four homogeneous layers and a topography with small-scale variations. As can be clearly seen from Figure 1, the reflection events are, due to the topography, far from being hyperbolic. A direct application of a second-order stacking operator within a reasonable aperture will most likely fail—static corrections and/or redatuming would have to be applied before.

With the help of the wavefield attributes, the second-order traveltimes approximation can be generalized to contain traveltimes corrections that depend on the source and receiver elevations (Zhang et al., 2002). The number of wavefield attributes remains the same, no additional search is required. Although the CRS operator (red surface in Figure 1) is still based on a second-order approximation, it takes a rather complicated form and adapts well to the reflection event. As a consequence, the stacked section (Figure 2a) represents a ZO simulation of high quality, still attached to the actual topography.

The wavefront attributes and the associated traveltimes derivatives are obtained as if the data were recorded on a plane surface with floating datum. Thus, most of the complexity introduced by the topography is

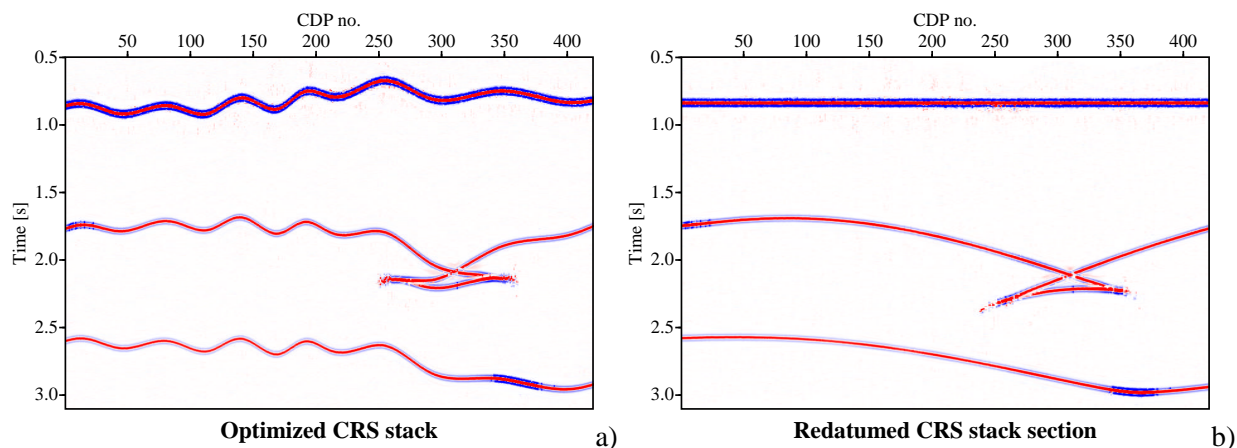


Figure 2: ZO section simulated for a four layer model with topography a) without and b) with redatuming based on the wavefield attributes. The redatumed section is equivalent to the same data forward-calculated without topography.

already removed in the attributes. This allows to apply a redatuming to a plane datum, almost without additional effort: the redatumed section in Figure 2b) is indeed a good approximation of the ZO section forward-calculated *without* topography.

Conclusions. We reviewed the basic concepts of second-order traveltimes approximations and their application in data-driven seismic reflection imaging. With the assumption of a known and (locally) constant near-surface velocity, a link between the spatial first and second derivatives of the traveltimes and the spatial properties of wavefronts, called kinematic wavefield attributes, can be established that allow a variety of applications. We showed two examples of the use of these concepts: the generalization of the second-order traveltimes approximation of the CRS stack to situations with topography and the redatuming of the stack result to a plane datum. These generalizations are not possible without the (implicit or explicit) move from traveltimes derivatives to spatial wavefront properties and, thus, clearly demonstrate the advantage of this concept.

Acknowledgments

We would like to thank the sponsors of the *Wave Inversion Technology Consortium* for their support.

References

- Berkovitch, A., Gelchinsky, B., and Keydar, S. (1994). Basic formulae for multifocusing stack. In *Extended Abstracts*, 56th Mtg. Eur. Assoc. Expl. Geophys. Session: P140.
- Biloti, R., Santos, L. T., and Tygel, M. (2002). Multiparametric traveltimes inversion. *Stud. geophys. geod.*, 46:177–192.
- Duveneck, E. (2003). Determination of velocity models from data-derived wavefront attributes. In *Extended Abstracts*, 65th Mtg. Eur. Assn. Geosci. Eng. EAGE.
- Höcht, G., de Bazelaire, E., Majer, P., and Hubral, P. (1999). Seismics and optics: hyperbolae and curvatures. *J. Appl. Geoph.*, 42(3,4):261–281.
- Landa, E., Gurevich, B., Keydar, S., and Trachtman, P. (1999). Application of multifocusing method for subsurface imaging. *J. Appl. Geoph.*, 42(3,4):283–300.
- Schleicher, J., Tygel, M., and Hubral, P. (1993). Parabolic and hyperbolic paraxial two-point traveltimes in 3D media. *Geophys. Prosp.*, 41(4):495–514.
- Zhang, Y., Höcht, G., and Hubral, P. (2002). 2D and 3D ZO CRS stack for a complex top-surface topography. In *Extended Abstracts*, 64th Mtg. Eur. Assn. Geosci. Eng., Session P166.